

# Structural Study of Poly(phenylsilsesquioxane) Sol–Gel Materials

M. Smaihi\*,† and T. Jermoumi

Laboratoire des Matériaux et Procédés Membranaires, UMR 9987 CNRS, ENSCM, UMII 8, rue de l'École Normale, 34053 Montpellier Cedex 1, France

J. Marignan

Groupe de Dynamique des Phases Condensées, CNRS URA 233, USTL CC026, Place Eugène Bataillon, 34095 Montpellier Cedex 5, France

Received March 30, 1995. Revised Manuscript Received October 5, 1995\*

Gels have been prepared via the sol–gel process by cohydrolysis of an organoalkoxide of the type  $R_nSi(OR')_{4-n}$  and tetramethoxysilane. The influence of organoalkoxide functionality and concentration on the resulting gel structure has been studied using two organoalkoxysilanes: diphenyldimethoxysilane and phenyltrimethoxysilane. Phenyltrimethoxysilane–tetramethoxysilane and diphenyldimethoxysilane–tetramethoxysilane gels structures have been studied by solid-state NMR, small-angle X-ray scattering, and differential scanning calorimetry. The interconnection of the networks provided by the organoalkoxysilanes and tetramethoxysilane has been demonstrated. NMR and SAXS analysis showed that hybrid gels obtained with the trifunctional alkoxide are more condensed than the difunctional hybrid gels. The scattering experiments demonstrate the absence of any heterogeneities in the range 10–100 Å. These materials have a unique glass transition temperature that indicates the existence of a homogeneous network.

## 1. Introduction

The sol–gel process provides a versatile approach to the preparation of hybrid organic–inorganic networks.<sup>1–7</sup> Low-temperature chemistry, based on inorganic polymerization,<sup>8–9</sup> introduces organic molecules within an inorganic network and adjusts the degree of interpenetration of organic and inorganic components from the submicron range down to the nanoscale.

The first example of a polymer–metal oxide hybrid material prepared via a sol–gel reaction was the hard contact lens material reported by Scholze and Schmidt.<sup>1–2</sup> Hard contact lenses require mechanical toughness, transparency, oxygen permeability, and wettability of the surface to prevent adhesion of proteins in tears. The presence of dimethylsiloxane and hydroxy groups enhances oxygen permeability and wettability. A large variety of hybrid materials have been created in which organic molecules play different roles such as improving the characteristics of the matrices (modification of the mechanical properties,<sup>10–12</sup> porosity control, adjustment

of the hydrophilic/hydrophobic balance<sup>13,14</sup>) or to provide a particular chemical, physical or biochemical property (modulation of the optical index,<sup>15–16</sup> chemical or biochemical reactivity,<sup>17–20</sup> luminescent properties.<sup>21</sup>).

The preparation of sol–gel-derived organically modified silicates basically follows the same initial steps as for general sol–gel processes, hydrolysis, and condensation. Differences occur in the effect of reaction rates as a function of the organic ligands which determines the structural properties of the final material. The preparation of true hybrid materials with a mixture of organic and inorganic groups at the molecular level can best be achieved by using chemically modified alkoxides  $R'_xM(OR)_{n-x}$ . The Si–C bond, highly stable with respect to hydrolysis, is the basis for development of hybrid organic–inorganic gels containing silicon. Therefore the ligand R acts as a network modifier in the resulting structure.

\* Temporary address: Department of Chemical Engineering, University of Colorado, Boulder, CO 80309-0424.

† Abstract published in *Advance ACS Abstracts*, November 15, 1995.

- (1) Scholze, H. *J. Non-Cryst. Solids* **1985**, *73*, 669.
- (2) Schmidt, H. *J. Non-Cryst. Solids* **1985**, *73*, 681.
- (3) Huang, H. H.; Orlor, B.; Wilkes, G. L. *Macromolecules* **1987**, *20*, 1322.
- (4) Mackenzie, J. D.; Chung, Y. J.; Hu, Y. *J. Non-Cryst. Solids* **1992**, *147–148*, 271.
- (5) Dire, S.; Babonneau, F.; Sanchez, C.; Livage, J. *J. Mater. Chem.* **1992**, *2*, 239.
- (6) Survivet, F.; Lam, T. M.; Pascault, J. P.; Pham, Q. T. *Macromolecules* **1992**, *25*, 4309.
- (7) Wei, Y.; Yang, D.; Tang, L. *J. Mater. Res.* **1993**, *8*, 1143.
- (8) Brinker, C. J.; Scherer, G. *Sol-gel Science, the Physics and Chemistry of Sol-gel Processing*; Academic Press: San Diego, 1989.
- (9) Livage, J.; Henry, M.; Sanchez, C. *Prog. Solid State Chemistry* **1988**, *18*, 259.

- (10) Wilkes, G. L.; Orlor, B.; Huang, H. H. *Polym. Prepr.* **1985**, *26*, 300.
- (11) Sur, G. S.; Mark, J. E. *Eur. Polym. J.* **1985**, *21* (12), 1051.
- (12) Morikawa, A.; Iyoku, Y.; Kakimoto, M.; Imai, Y. *J. Mater. Chem.* **1992**, *2*, 679.
- (13) Izumi, K.; Tanaka, H.; Murakami, M.; Degushi, T.; Morita, A.; Toghe, N.; Minami, T. *J. Non Cryst. Solids* **1990**, *121*, 344.
- (14) Chojo, Y.; Saegusa, T. *Adv. Polym. Sci.* **1992**, *100*, 11.
- (15) Schmidt, H.; Seiferling, B. *Mater. Res. Soc. Symp. Proc.* **1986**, *73*, 739.
- (16) Wang, B.; Wilkes, G. L.; Schmidt, C. D.; McGrath, J. E. *Polym. Commun.* **1991**, *32*, 400.
- (17) Elerby, L. M.; Nishida, C. R.; Nishida, F.; Namayaka, S. A.; Dunn, B.; Valentine, J. S.; Zink, J. I. *Science* **1992**, *255*, 1113.
- (18) Audebert, P.; Demaille, C.; Sanchez, C. *Mater. Chem.* **1993**, *5*, 911.
- (19) Collino, R.; Therasse, J.; Chaput, F.; Boilot, J. P.; Levy, Y. In *Better Ceramics through Chemistry VI*, Mat. Res. Soc. Symp. Proc. 346; Cheetham, A. K.; Brinker, C. J., Mearns, M. L., and Sanchez, C., Eds.; MRS: Pittsburgh, PA, 1994; p 1033.
- (20) Zink, J. I.; Valentine, J. S.; Dunn, B. *New J. Chem.* **1994**, *18*, 1109.
- (21) Dire, S.; Babonneau, F.; Sanchez, C.; Livage, J. *J. Mater. Chem.* **1992**, *2*, 239.

$^{29}\text{Si}$  liquid-state NMR has been performed to follow the hydrolysis–condensation reactions of various systems: poly(dimethylsiloxane)–tetraethoxysilane (PDMS–TEOS),<sup>22</sup> phenyltrimethoxysilane–tetramethoxysilane (PTMOS–TMOS) and diphenyldimethoxysilane–tetramethoxysilane (DPMOS–TMOS),<sup>23</sup> diethyldiethoxysilane–tetramethoxysilane (DEDMS–TMOS)<sup>24,25</sup> and methyltriethoxysilane–tetraethoxysilane (MTES–TEOS).<sup>26,27</sup> In some of these studies, evidence of co-condensation between the alkoxides has been proved by the presence of new peaks in the spectra corresponding to T–Q or D–Q species. The copolymerization of DEDMS with various M–(OR)<sub>n</sub> alkoxides has been studied.<sup>28</sup> A large variety of these materials have been prepared, but there has been not much evaluation of their structure. Small-angle X-ray scattering (SAXS) and thermomechanical techniques have been used to study the structure of poly(tetramethylsiloxane)–tetraethoxysilane (PTMO–TEOS)<sup>29,30</sup> and PDMS–TEOS<sup>3,10,31–33</sup> networks;  $^{29}\text{Si}$  MAS NMR has been used to study DEDMS–TEOS materials.<sup>24,25</sup> A cluster model<sup>29</sup> has been suggested to describe these materials.

This paper presents a study of the molecular structure of two hybrid gels obtained with organoalkoxysilanes with lower functionality than the tetramethoxysilane: phenyltrimethoxysilane  $\text{C}_6\text{H}_5\text{Si}(\text{OCH}_3)_3$  (abbreviated PTMOS) with a functionality of three and diphenyldimethoxysilane  $(\text{C}_6\text{H}_5)_2\text{Si}(\text{OCH}_3)_2$  (abbreviated DPMOS) with a functionality of two. The presence of the phenyl side groups confers thermal stability, hydrophobicity, and flexibility to the films. Gels were prepared by cohydrolysis of DPMOS or PTMOS and TMOS. In each mixture (DPMOS–TMOS or PTMOS–TMOS), various proportions of organo alkoxide have been introduced in order to evaluate the concentration effect of difunctional and trifunctional organoalkoxides on the structure. Solid-state  $^{29}\text{Si}$  nuclear magnetic resonance (NMR) has been performed to characterize the formation of hybrid siloxane networks and their molecular structure. Small-angle X-ray scattering (SAXS) has been used to study the gels' structure and differential

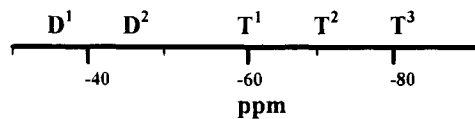


Figure 1. Chemical shift ranges of D and T species.

scanning calorimetry (DSC) to characterize the homogeneity of the networks by the glass temperature transitions.

## 2. Experimental Section

**2.1. Preparation of Samples.** DPMOS and PTMOS (Dynamit Nobel) and methyl alcohol (Merck) were used as received. The  $^{29}\text{Si}$  NMR spectra of the pure alkoxides contain a single peak at  $-30.07$  and  $-55.33$  ppm, respectively, for DPMOS and PTMOS. These spectra do not show the presence of hydrolyzed or modified species. Deionized water (18 M $\Omega$ ) was used for the hydrolysis.

For the preparation of the sols, a mixture of methanol and water was slowly poured into a mixture of precursors and methanol. The homogeneity of the solution was checked after stirring for 10 min at room temperature. The aging of the solutions was performed in closed glass containers at room temperature. The macroscopic gel time ( $t_g$ ) was defined by observing the stiffness after tilting the container. During gelation, no significant change of volume was noted and transparent gels were obtained.

DPMOS–TMOS gels have been obtained with a hydrolysis ratio ( $\text{H}_2\text{O}/\text{OR}$ ) of 0.3 and a silicon concentration of 3 mol/L. The organoalkoxide proportion (DPMOS/[DPMOS + TMOS]) ranges from 0.03 to 0.64. PTMOS–TMOS gels have been obtained with a hydrolysis ratio of 0.5 and a silicon concentration of 3 mol/L. The organoalkoxide proportion can be varied from 0.04 to 0.9.

This study requires reference gels for each alkoxide. Reference gels have been prepared under the same conditions as the hybrid systems, the only difference being that the second alkoxide has been replaced by an equal volume of alcohol. Thus the concentrations remain the same.

**2.2.  $^{29}\text{Si}$  NMR.** The molecular structure of the solid gels was obtained from 59.62 MHz  $^{29}\text{Si}$  NMR spectra recorded on a Bruker MSL 300 spectrometer by using the magic angle spinning (MAS) technique. The spectra were obtained with a pulse of 5.8  $\mu\text{s}$  (pulse angle: 60°), repetition time of 20 s, and 1500 transients were accumulated before Fourier transformation. These conditions have been checked for quantitative analysis of the spectra. The spectra width was 15 kHz; 16 000 data points were used. The samples were put in an alumina rotor which was rotated at 5 kHz. All samples were kept at a constant temperature of 21 °C throughout the experiment. The chemical shifts are given with reference to tetramethylsilane (TMS).

Classical notation D and T was used for the different silicate species depending on the number of carbon and oxygen bridging atoms;  $i$  indexes represent the number of oxo bridges. D<sup>*i*</sup> is used for species which have two phenyl side groups and  $i$  siloxane bridges ( $i = 0, 1, \text{ or } 2$ ). In the same manner, T<sup>*i*</sup> denotes species that have one phenyl side group and  $i$  siloxane bonds. Literature references<sup>34–36</sup> provide information on the average chemical shift ranges of D<sup>1</sup>, D<sup>2</sup>, T<sup>1</sup>, T<sup>2</sup>, and T<sup>3</sup> species; they are sketched in Figure 1 (with reference to tetramethylsilane or TMS). The relative proportion of the D<sup>*i*</sup> (T<sup>*i*</sup>) species will be used, calculated on the basis of the experimental spectra.

**2.3. Differential Scanning Calorimetry (DSC).** Calorimetric analysis was performed on a Perkin Elmer DSC4

(22) Iwamoto, T.; Morita, K.; Mackenzie, J. D. *J. Non-Cryst. Solids* **1993**, *159*, 65.

(23) Jermoumi, T.; Smaihhi, M.; Hovnanian, N. *J. Mater. Chem.* **1995**, *5*, 1203–1208.

(24) Bois, L.; Ph.D. Thesis, Paris VI University, 1993.

(25) Babonneau, F.; Bois, L.; Livage, J. In *Better Ceramics through Chemistry V*; Mat. Res. Soc. Symp. Proc. 271; Hampden-Smith, M. J., Klemperer, W. G., Brinker, C. J., Eds.; MRS: Pittsburgh, PA, 1992; p 237.

(26) Sugahara, Y.; Tanaka, Y.; Sato, S.; Kuroda, K.; Kato, C. In *Better Ceramics through Chemistry V*; Mat. Res. Soc. Symp. Proc. 271; Hampden-Smith, M. J., Klemperer, W. G., Brinker, C. J., Eds.; MRS: Pittsburgh, PA, 1992; p 231.

(27) Prabakar, S.; Assink, R. A.; Raman, N. K.; Brinker, C. J. In *Better Ceramics through Chemistry VI*; Mat. Res. Soc. Symp. Proc. 346; Cheetham, A. K., Brinker, C. J., Mcartney, M. L., Sanchez, C., Eds.; MRS: Pittsburgh, PA, 1994; p 979.

(28) Dire, S.; Babonneau, F.; Sanchez, C.; Livage, J. *J. Mater. Chem.* **1991**, *2*, 239.

(29) Huang, H. H.; Glaser, R. H.; Wilkes, G. L. In *Inorganic and Organometallic Polymers*; Zeldin, M., Wynne, K. J., Allcock, H. R., Eds.; ACS Symp. Ser. **1988**, *360*, 354.

(30) Krakovsky, I.; Urakawa, H.; Ikeda, Y. *Bull. Inst. Chem. Res., Kyoto Univ.* **1994**, *72*, 231.

(31) Huang, H. H.; Orlor, B.; Wilkes, G. L. *Polym. Bull.* **1985**, *14*, 557.

(32) Wilkes, G. L.; Orlor, B.; Huang, H. H. *ACS Polym. Prepr.* **1985**, *26*, 300.

(33) Huang, H. H.; Wilkes, G. L.; Carlson, J. G. *Polym.* **1989**, *30*, 2001.

(34) Kintzinger, J. P.; Marsmann, H. *NMR 17: Oxygen 17 and Silicon 29*; Diehl, P., Fluck, E., Kosfeld, R., Eds.; Springer-Verlag: Berlin, 1981.

(35) Engelhardt, G.; Jancke, H.; Lippmaa, E.; Samoson, A. *J. Organomet. Chem.* **1981**, *210*, 295.

(36) Engelhardt, G.; Mñgi, M.; Lippmaa, E. *J. Organomet. Chem.* **1973**, *54*, 115.

**Table 1. Gel Time (days) of Gels of Different Compositions in the DPMOS–TMOS and PTMOS–TMOS Systems**

organoalkoxide molar proportion	0.03	0.09	0.18	0.54	0.6	0.8	0.9
$T$ (DPMOS–TMOS) (days)	2.5	10	26	175	300		
$T$ (PTMOS–TMOS) (days)	1	1.5	2	5	17	26	28

apparatus to study the glass transition temperature and homogeneity of those hybrid systems. The glass transition is characterized by an endothermic signal induced by chain segment mobility. Two types of experiment have been performed on the hybrid gels. In the first, the samples have been cooled from 25 to  $-150$  °C at 40 °C/min and then heated at the same rate to 100 °C. In the second, the samples are heated from 25 to 500 °C at 40 °C/min and then cooled to 25 °C at the same rate. In order to avoid any artifact from water evaporation or other thermal events, the scans have been repeated after cooling, and all transitions have been noted during the second heating. Glass transition temperatures ( $T_g$ ) were measured at the midpoint of the discontinuity of the specific heat.

Thermogravimetric analysis has been also performed on the samples (heating rate of 40 °C/min in air) to appreciate the thermal stability of these gels and note the temperatures corresponding to eventual weight losses.

**2.4. Small-Angle X-ray Scattering (SAXS).** Numerous studies describe gel structures using fractal geometry<sup>37–40</sup> Sol-gel materials and, in particular, silica gels<sup>41,42</sup> have been described as systems which present fractal characteristics. The SAXS technique uses the electronic contrast between scattering particles to evaluate the fractal structure. The experiments have been performed on a low resolution instrument. The data were collected using a position-sensitive detector and a slit collimation system. The scattering curves were de-smearred using two methods: an iterative method<sup>43</sup> and another method proposed by Strobl<sup>44</sup> which determines the inverse of the apparatus function. Both procedures gave the same result. The samples were put into a glass capillary (diameter 1 mm). The incident wavelength is 1.54 Å ( $\lambda$  Cu  $K\alpha_1$ ). These experimental parameters allows studies in a range of wave vectors from 0.01 to 1 Å<sup>-1</sup>. The middle part of the scattering curve  $I(Q) = f(Q)$  corresponds to the fractal regime where the scattered intensity is  $I(Q) = Q^{-D}$ . The mass fractal dimension was obtained by fitting the deconvoluted spectra with the structure factor proposed by Teixeira<sup>45</sup> where the adjustable parameters are the correlation length (a cutoff introduced in the pair correlation function which can be seen as the size of the fractal aggregates) and the fractal dimension. This result has been obtained for hybrid gels for various compositions of our hybrid gels.

### 3. Results

The comparison of these two materials shows that gel time is much shorter for PTMOS solutions than DPMOS solutions (Table 1). This can be explained by the fact that trifunctional alkoxides can build a three dimensional network, whereas a bifunctional alkoxide leads



**Figure 2.** <sup>29</sup>Si NMR spectra of various DPMOS–TMOS gels compositions (numbers indicate molar ratio of DPMOS).

to linear chains. Thus the materials formed by these inorganic polymers do not have the same molecular structure.

**3.1. Solid-State <sup>29</sup>Si NMR.** Hybrid gels DPMOS–TMOS and PTMOS–TMOS have been studied and compared as a function of their organo alkoxide proportion. Although it is not easy to distinguish subtle details in the molecular structure, it is sufficient to separate and evaluate quantitatively the relative contributions of the silicon atoms with 0, 1, 2, or 3 siloxane bridges. The species formed during the condensation reactions have been identified and their quantitative evolution calculated.

**(A) DPMOS–TMOS Hybrid Gels.** The NMR spectra corresponding to gels of various compositions are presented in Figure 2. The resonance peaks are situated in two regions corresponding to the signals of DPMOS and TMOS species. The chemical shifts of  $D^i$  species ( $D^1$  and  $D^2$ ) range between  $-25$  and  $-50$  ppm, and the resonance peaks of the  $Q^i$  species ( $Q^2$ ,  $Q^3$ ,  $Q^4$ ) are situated between  $-85$  and  $-110$  ppm. The comparison of these spectra shows that the chemical shift of the  $Q^4$  units varies significantly with composition, while all other resonance peaks are equivalent with respect to composition.

Figure 3 presents the  $Q^4$  resonance peak position as a function of the proportion of DPMOS in the hybrid gels and the position of the same units in the references. The  $Q^4$  species chemical shift in the hybrid gels varies continuously with composition (3 to 63%) over a 3 ppm range, from  $-110$  to  $-107$  ppm. Thus this  $Q^4$  species downfield gives a first indication of the formation of interconnected Q–D sites. This shift may originate from a change in the Si–O–Si bond angle induced by Q–D bond formation which modifies the site geometry.

(37) Schaefer, D. W.; Keefer, K. D. *Mater. Res. Symp. Proc.* **1986**, 73, 277.

(38) Orcel, G.; Gould, R. W.; Hench, L. L. *Mater. Res. Soc. Symp. Proc.* **1986**, 73, 289.

(39) Pope, E. J. A. In *Better Ceramics through Chemistry V*; Mat. Res. Soc. Symp. Proc. 271; Hampden-Smith, M. J., Klempner, W. G., Brinker, C. J., Eds.; MRS: Pittsburgh, PA, 1992, p 213.

(40) Pouxviel, J. C.; Boilot, J. P.; Smahli, M.; Dager, A. *J. Non-Cryst. Solids* **1988**, 106, 147.

(41) Keefer, K. D. *Mater. Res. Soc. Symp. Proc.* **1986**, 73, 295.

(42) Keefer, K. D.; Schaefer, D. W. *Phys. Rev. Lett.* **1986**, 56, 2376.

(43) Lake, J. A. *Acta Crystallogr.* **1967**, 23, 191.

(44) Strobl, G. R. *Acta Crystallogr.* **1970**, A26, 367.

(45) Teixeira, J. *J. Appl. Crystallogr.* **1988**, 21, 781.

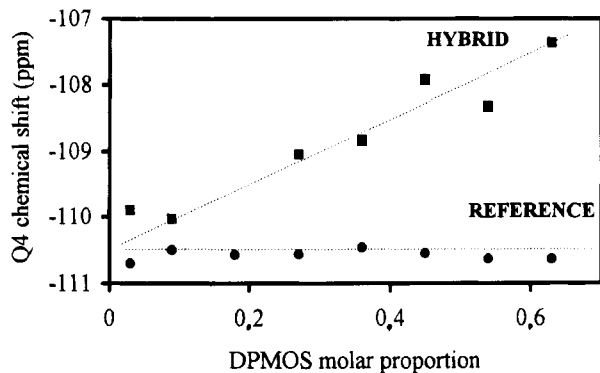


**Figure 3.**  $Q^4$  species chemical shift in DPMOS–TMOS gels as a function of the DPMOS proportion in the gels.

Previous studies<sup>46,47</sup> show that there is a correlation between  $^{29}\text{Si}$  chemical shift and the electronegativity in the SiO bonds. A quantum-chemical model<sup>48</sup> demonstrate a correlation between  $^{29}\text{Si}$  chemical shifts and mean SiOSi bond angles. The continuous variation of the shift shows that this angle variation increases continuously when the DPMOS proportion in the gel increases.

The comparison of the chemical shifts observed in hybrid gels with those of reference gels shows that this downfield shift is only observed for  $Q^4$  units. All other  $Q^i$  species ( $Q^2$  and  $Q^3$ ) present resonance peaks similar to the references:  $Q^2$  species chemical shift is constant and identical to the reference ( $-91.5$  ppm) and  $Q^3$  species vary from  $-100.6$  to  $-100.1$  ppm while the reference is situated at  $-101$  ppm. The same statement can be made concerning the D species: their resonances in the hybrid gels are similar to those observed in the reference ( $-36.8$  and  $-43.3$  ppm for respectively  $D^1$  and  $D^2$  units).

The network density has been evaluated by a quantitative analysis of the different  $Q^i$  and  $D^i$  species. Figure 4 presents the relative proportion of  $D^i$  and  $Q^i$  species as a function of the DPMOS molar proportion. In the hybrid networks,  $D^2$  sites are always in the majority whatever the gel composition (Figure 4a) and they increase from 60 to 70% with the DPMOS molar proportion. Concerning the Q species (Figure 4b), there is no significant variation of the  $Q^i$  units relative proportion:  $Q^4$  sites are always in the majority (55%) and relative proportions of  $Q^3$  and  $Q^2$  species are equal to 30% and 15%, respectively.

The comparison of hybrid and reference gels shows that these species distributions are significantly different in the reference gels. The major D species present in the reference gels is  $D^1$  (60%), while the relative proportion of  $Q^4$  is lower in the hybrid systems than in the corresponding reference gel. This shows that the presence of D sites induces a decrease in Q species condensation while at the same time the TMOS introduction induces an increase in  $D^i$  species condensation.

(B) *PTMOS–TMOS Hybrid Gels.* Spectra of various compositions are represented in Figure 5. The resonance peaks are situated in two regions corresponding to PTMOS and TMOS species. Chemical shifts of  $T^i$

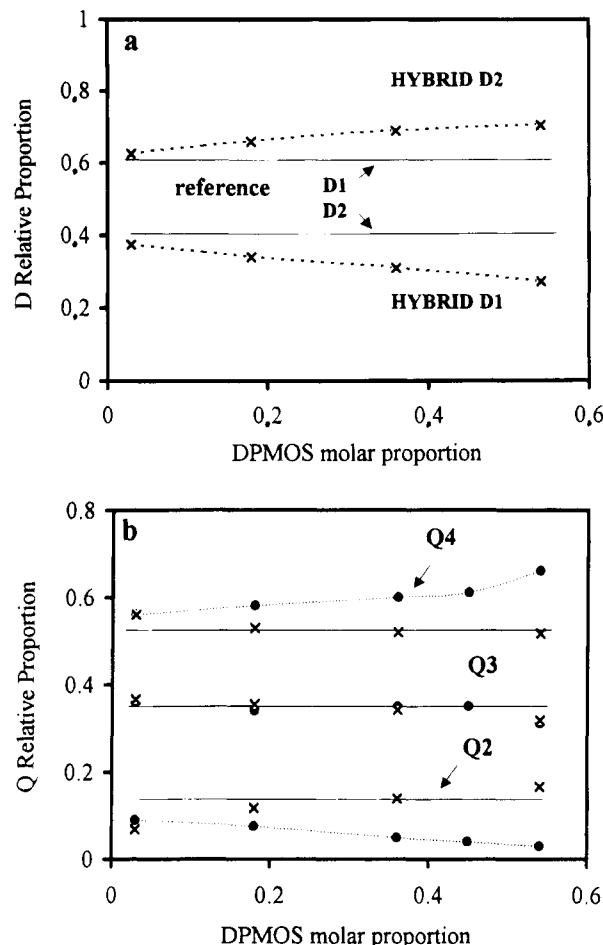


**Figure 4.** Relative concentration of  $D^i$  (a) and  $Q^i$  (b) species in DPMOS–TMOS gels as a function of DPMOS proportion (● are the reference points and × are the hybrid points).

species ( $T^1$ ,  $T^2$ , and  $T^3$ ) range from  $-55$  to  $-80$  ppm. The  $Q^i$  species are situated between  $-85$  and  $-110$  ppm.

In both hybrid and reference gels, the  $Q^2$  and  $Q^3$  species chemical shifts are constant whatever the composition and equal respectively  $-91$  and  $-101$  ppm.  $T^1$  and  $T^2$  species in the references show peaks at  $-62$  and  $-70$  ppm, respectively. In the hybrid gels these chemical shifts have a tendency to decrease by 1 ppm over the range of composition.

The most important variation between hybrid gels and references is observed for  $Q^4$  and  $T^3$  species. Figure 6 represents the variations in the hybrid gels and the references as a function of composition. The  $Q^4$  chemical shifts (Figure 6a) increase continuously from  $-110$  to  $-108$  ppm in the hybrid systems while it stays constant at  $-110$  ppm in the reference. On the other hand,  $T^3$  species chemical shift variation (Figure 6b) increases continuously from  $-79$  to  $-77$  ppm in the hybrid gels while their resonance peak is constant at  $-80$  ppm in the reference. Thus, as the proportion of PTMOS in the gel increases, the  $Q^4$  species chemical shift is shifted downfield. This shift may be induced by changes in the Si–O–Si bond angle due to Q–T bondings which increase with the PTMOS proportion. Moreover, the variation of the  $T^3$  species position shows that the Si–O–Si bond angles are modified by the presence of Q entities. This behavior shows that the cohydrolysis of TMOS and PTMOS leads to the formation of an interconnected network of  $T^3$  and  $Q^4$  sites.

(46) Engelhardt, G.; Radeglia, R. *Chem. Phys. Lett.* **1984**, *108*, 271.

(47) Smith, J. V.; Blackwell, C. S. *Nature* **1983**, *303*, 223.

(48) Radeglia, R.; Engelhardt, G. *Chem. Phys. Lett.* **1985**, *114*, 28.

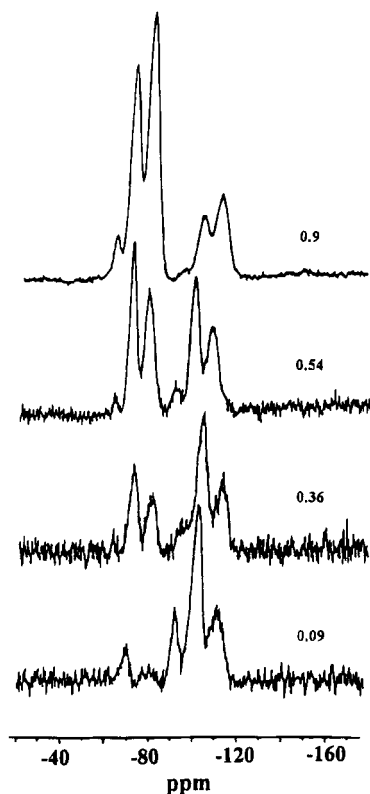


**Figure 5.**  $^{29}\text{Si}$  NMR spectra of various PTMOS-TMOS gel compositions (numbers indicate molar ratio of PTMOS).

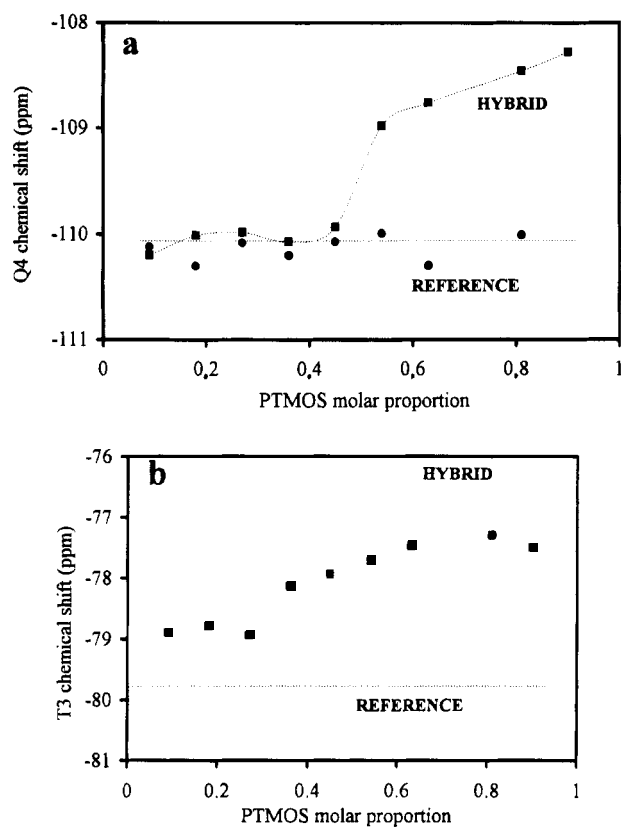


**Figure 6.**  $\text{Q}^4$  (a) and  $\text{T}^3$  (b) species chemical shift in PTMOS-TMOS gels as a function of the PTMOS proportion in the gels.

The quantitative study of different  $\text{T}^i$  species distributions provides information on the compactness of these networks. In the hybrid gels, there is no variation with gel composition:  $\text{T}^3$  species are in majority (0.7);  $\text{T}^1$  and  $\text{T}^2$  species relative proportions are equal to 0.06 and

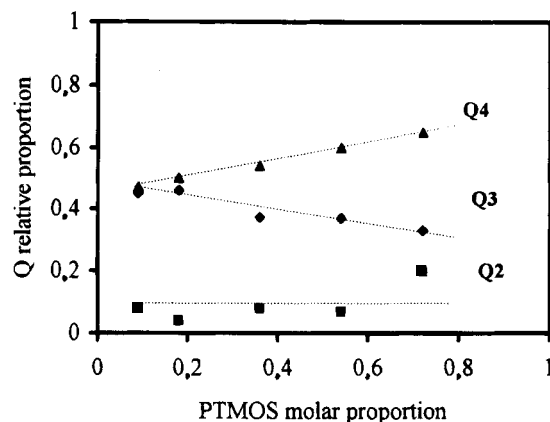


**Figure 7.** Relative concentration  $q^n$  of  $\text{Q}^n$  species in PTMOS-TMOS gels as a function of PTMOS proportion.

0.24, respectively. In the PTMOS reference gels, the  $\text{T}^3$  and  $\text{T}^2$  relative proportions are equal to 0.3 and 0.7, respectively. This demonstrates the influence of TMOS condensation on the PTMOS condensation. Concerning the  $\text{Q}^i$  species, similar behavior is observed in the hybrid and the reference gels. Figure 7 presents the  $\text{Q}^i$  species relative proportion variation as a function of the PTMOS molar proportion. The  $\text{Q}^2$  species relative proportion is constant (0.05);  $\text{Q}^3$  decreases while  $\text{Q}^4$  increases. This shows that the TMOS condensation is not substantially influenced by the presence of the trifunctional alkoxide.

The NMR study of DPMOS-TMOS and PTMOS-TMOS systems showed that the  $\text{Q}^4$  units and  $\text{T}^3$  units are significantly shifted toward the low field in these networks while D species do not seem to be influenced by the presence of other adjacent species. Similar studies on dimethyldiethoxysilane-tetraethoxysilane (DMDES-TEOS) systems<sup>28,29</sup> showed that both Q and D units display a chemical shift variation. The particular behavior of the phenyl D units may be explained by the steric hindrance of the phenyl groups which makes the D units completely isolated from the influence of their neighbors while T species containing only one phenyl are still able to respond to the presence of Q units. As D units formed by DMDES are almost of the same size as Q units, they may then have the same behavior (from the chemical shift point of view) as the Q units. However, the Q downfield shifts observed in the phenylsilsesquioxane materials may demonstrate the existence of a chemical bond between the TMOS and the organoalkoxysilane. Moreover, the quantitative NMR study showed that the introduction of TMOS contributes to a better organoalkoxysilane condensation, whereas the condensation of TMOS itself depends on the functionality of the organoalkoxide. In the DPMOS-TMOS materials, the Q species condensation decreases with the concentration of DPMOS showing the influence of the steric hindrance of the phenyl groups. For the PTMOS-TMOS gels, the TMOS condensation is not influenced by the presence of the PTMOS aromatic group.

**3.2. Differential Scanning Calorimetry.** Figure 8 presents a typical TGA curve obtained on a nonpreheated DPMOS-TMOS gel ( $x = 0.36$ ). TGA experiments gave the same results for all samples showing that they are thermally stable until 500 °C. Weight-loss occurring below 100 °C correspond to water evaporation, and the small weight loss (7%) observed between

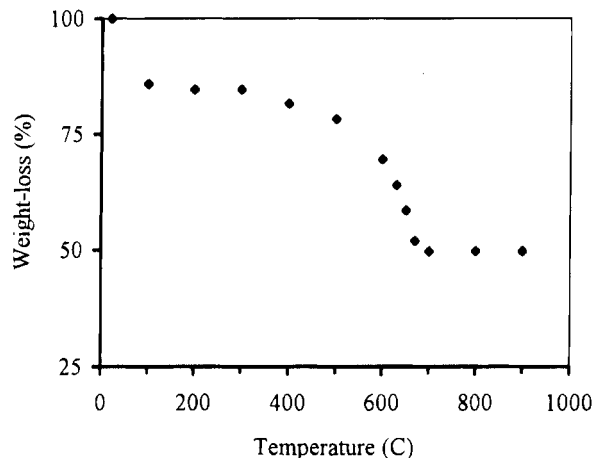


**Figure 8.** TGA curve (40 °C/min in air) of DPMOS-TMOS sample (36% of DPMOS).

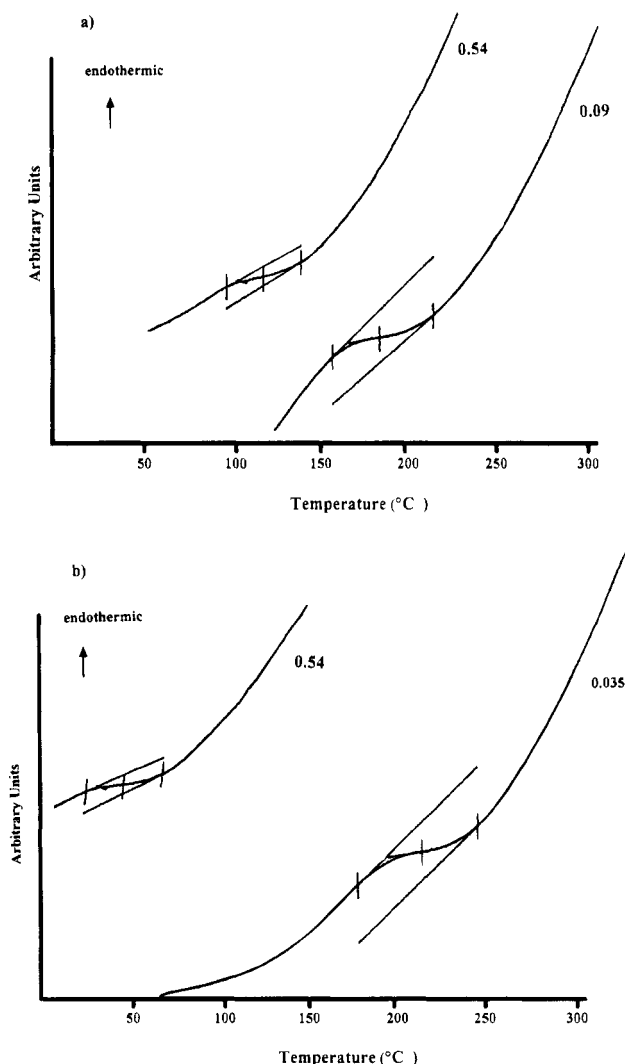


**Figure 9.** DSC curves of PTMOS-TMOS (a) and DPMOS-TMOS (b) samples of different compositions (numbers indicate organoalkoxide molar ratio).

100 and 500 °C is related to the loss of organic volatiles. Figure 9 presents the DSC curves of PTMOS-TMOS and DPMOS-TMOS preheated samples for two compositions of each system. All curves show the same shape with a well defined glass transition step. The glass temperature variations are presented in Figure 10.  $T_g$  decreases with an increase in the organoalkoxide pro-

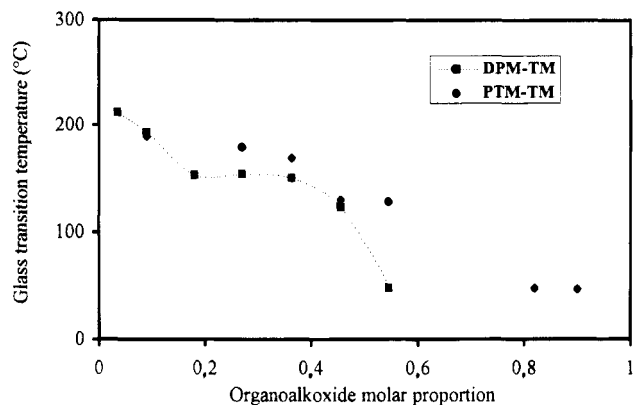


**Figure 10.** Glass transition temperatures of DPMOS-TMOS and PTMOS-TMOS gels as a function of the organoalkoxide proportion in the gel.

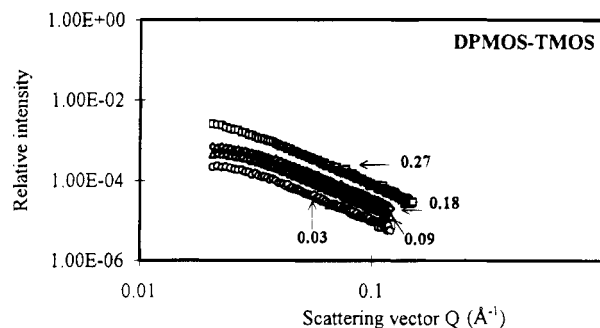


**Figure 11.** X-ray intensity profiles  $I(Q) = f(Q)$  of various DPMOS-TMOS gels compositions.

portion in the material. For the DPMOS-TMOS gels, the glass transition temperature decreases from 212 to 32 °C as the DPMOS proportion varies from 3 to 54%. For PTMOS-TMOS,  $T_g$  decreases from 189 to 47 °C as the proportion of PTMOS increases from 9 to 90%. The glass transition temperature of the DPMOS and PTMOS reference gels are situated at 1 and 30 °C, respectively. Thus the hybrid gels glass transitions are higher than those of their reference. As mobility restrictions of the polymeric chains result in an increase of the glass transition temperature,<sup>43</sup> these results show that the introduction of TMOS induces a more condensed network.

Dynamic mechanical and calorimetric studies have been made on other types of hybrid materials to study the mobility of the networks.<sup>29,49-51</sup> Depending on the homogeneity of the network, one to three glass transitions have been found corresponding to the different phases existing in the materials. Thus, the presence of a unique glass transition temperature demonstrates the homogeneity at a molecular level of the hybrid gels.

**3.3 Small-Angle X-ray Scattering.** Compositions with 3, 9, 18, and 27% of organoalkoxide have been studied. The corresponding scattering curves are presented in Figures 11 and 12, respectively, for DPMOS-TMOS and PTMOS-TMOS hybrid gels. The absence

(49) Parkhurst, C. S.; Doyle, W. F.; Silverman, L. A.; Singh, S.; Andersen, M. P.; McClurg, D.; Wnek, G. E.; Uhlmann, D. R. *Mater. Res. Soc. Symp. Proc.* **1986**, *73*, 769.

(50) Judeinstein, P.; Brik, M. E.; Bayle, J. P.; Courtieu, J.; Rault, J. In *Better Ceramics through Chemistry VI*; Mat. Res. Soc. Symp. Proc. **346**; Cheetham, A. K., Brinker, C. J., McCartney, M. L., Sanchez, C., Eds.; MRS: Pittsburgh, PA, 1994, p 937.

(51) Babonneau, F.; Maquet, J.; Dire, S. *Polym. Prepr.* **1993**, *34*, 242.

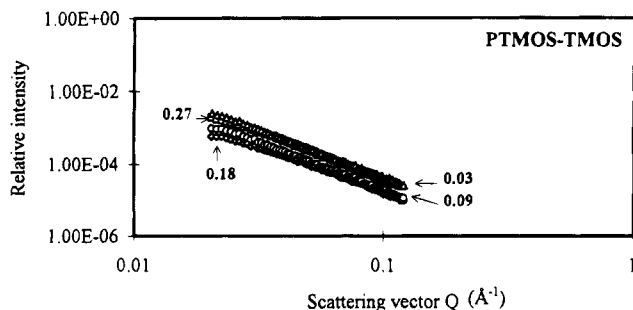


**Figure 12.** X-ray intensity profiles  $I(Q) = f(Q)$  of various PTMOS-TMOS gels compositions.

of any maximum in the Guinier region (low wave vector) indicates that there is no constructive interference corresponding to certain periodicity or heterogeneities and thus these materials are homogeneous in the range 10–100 Å. In DPMOS-TMOS systems, all curves have the same slope and the fractal dimension is equal to  $2.5 \pm 0.05$ . As their fractal dimension is equal, the compactness of these networks is similar. TMOS reference gels have fractal dimensions around  $2.7 \pm 0.05$ . Thus, whatever the composition, DPMOS-TMOS networks are more open than their reference.

In PTMOS-TMOS systems, the slopes are similar for all the samples and the fractal dimension equals  $2.7 \pm 0.05$ . The corresponding reference gels present scattering curves with a fractal dimension varying from 2.7 to 2.3 ( $\pm 0.05$ ). Thus the density of the PTMOS-TMOS hybrid gels is similar whatever the composition to the TMOS reference.

Although alkoxide-derived gels generally show a fractal dimension close to 2.1, some studies<sup>52,53</sup> found also fractal dimensions around 2.6–2.7.

Thus, DPMOS-TMOS gels fractal dimension (2.5) is lower than PTMOS-TMOS (2.7), showing that the networks formed with the trifunctional organoalkoxysilane are more dense.

#### 4. Conclusions

Phenyltrimethoxysilane-tetramethoxysilane and diphenyldimethoxysilane-tetramethoxysilane gels have been successfully prepared by the sol-gel process.

(52) Lebon, S.; Marignan, J.; Appell, J. *J. Non-Cryst. Solids* **1992**, *147–148*, 92.

(53) Molino, F.; Barthez, J. M.; Ayrat, A.; Marignan, J.; Guizard, C.; Jullien, R.; *Phys. Rev. E*, in press.

Their structures have been studied by solid-state NMR, small-angle X-ray scattering, and differential scanning calorimetry. The functional organoalkoxide DPMOS has two reactive bonds Si-OCH<sub>3</sub> which enables the formation of linear chains. On the other hand the three hydrolyzable bonds of the organoalkoxide PTMOS can build a three-dimensional network.

The chemical shift of the Q<sup>4</sup> species formed by the TMOS and T<sup>3</sup> species formed by PTMOS are shifted toward low field as the proportion of organoalkoxysilane increases in the gel while no shift is observed for the D species. Previous studies on DMDS-TEOS systems showed that both Q and D units show a variation in the chemical shift. This difference may be attributed to the steric hindrance of the phenyl groups which may protect the D units from the influence of the Q units. D units formed by DMDS present almost the same steric hindrance as Q units. Thus, the chemical shift variation observed for the phenyl hybrid networks should demonstrate the existence of Q-D and Q-T bonds.

The quantitative analysis of the different species contained in these hybrid networks shows that the presence of TMOS increases the organoalkoxysilane condensation. The influence of the phenyl group steric hindrance is demonstrated by the decrease of the Q network condensation with the DPMOS proportion in DPMOS-TMOS systems. Thus DPMOS-TMOS gels are less condensed than PTMOS-TMOS ones.

The homogeneity of these hybrid networks has been studied by small-angle X-ray scattering and differential scanning calorimetry. The scattering curves  $I = f(Q)$  demonstrate the absence of any heterogeneities in the region 10–100 Å. The fractal dimension is equal to 2.5 and 2.65, respectively, for DPMOS-TMOS and PTMOS-TMOS gels showing that the connectivity is greater when the organoalkoxysilane is trifunctional. Moreover these hybrid materials present a unique glass transition temperature which indicates the existence of a homogeneous network of interconnected Q and D (or T) sites. This temperature increases when the amount of organoalkoxysilane decreases showing the reinforcement of the network by the Q sites.

**Acknowledgment.** The authors gratefully acknowledge Prof. R. D. Noble for helpful discussions. M.S. wishes to thank NATO, who provided the opportunity for her stay in Boulder, CO.

CM950153Z